Author's personal copy

Remote Sensing of Environment 113 (2009) 2403–2411

Contents lists available at ScienceDirect

Remote Sensing of Environment

journal homepage: www.elsevier.com/locate/rse

Linking ecological information and radiative transfer models to estimate fuel moisture content in the Mediterranean region of Spain: Solving the ill-posed inverse problem

Marta Yebra *, Emilio Chuvieco

Department of Geography, University of Alcalá, Alcalá de Henares, Spain

ARTICLE INFO

Article history:
Received 16 April 2009
Received in revised form 22 June 2009
Accepted 2 July 2009

Keywords:
Live fuel moisture content
MODIS
Fire risk
Radiative transfer modelling

ABSTRACT

Live fuel moisture content (FMC) is a key factor required to evaluate fire risk and its operative and accurate estimation is essential for allocating pre-fire resources as a part of fire prevention. This paper presents an operative and accurate procedure to estimate FMC though MODIS (moderate resolution imaging spectrometer) data and simulation models. The new aspects of the method are its consideration of several ecological criteria to parameterize the models and consistently avoid simulating unrealistic spectra which might produce indetermination (ill-posed) problems when inverting the model. The methodology was operatively applicable to 12 shrubland plots located in different provinces of the Mediterranean region of Spain and tested with field data collected in those areas. The results showed that the proposed method efficiently tracks changes of FMC with average errors around 15%. However the model under-estimates FMC values higher than 135.68% since those situations were not included in the simulation scheme and the inversion precision is also dependent on an accurate estimation of LAI. These limitations will be overcome in future work mainly by including spectral signatures of vegetation with FMC values higher than 135.68% in the simulations, and by exploring new methods for LAI retrieval. Further efforts will also be devoted to extend this approach to other ecosystems.

© 2009 Elsevier Inc. All rights reserved.

1. Introduction

The estimation of plant water content from remotely sensed data has been extensively pursued in the last years (Ceccato et al., 2001, 2002; Cheng et al., 2006; Danson & Bowyer, 2004; Dennison et al., 2005; Garcia et al., 2008; Roberts et al., 2006; Stow et al., 2005; Yebra et al., 2008b; Zarco-Tejada et al., 2003). Many of these studies have aimed to provide an estimation of water stress conditions for fire risk assessment, since plant moisture increases the heat threshold to ignite a fuel and impedes fire propagation (Nelson, 2001). Fire risk evaluation is a critical part of fire prevention, since pre-fire planning resources require objective tools to monitor when and where a fire is more prone to occur, or when it will have more negative effects (Chuvieco et al., in press).

The measurement of plant water has been commonly approached using two parameters, the equivalent water thickness (EWT) and the fuel moisture content (FMC). The former refers to the amount of water by leaf area, while the latter by leaf dry mass. The former is more commonly estimated from remote sensing, since it is more associated to light absorption (Ceccato et al., 2001), while the latter is more common in the fire risk literature (Viegas et al., 1992). The two can be related through the dry matter content (DM, the amount of dry matter by leaf area), which also affects light absorption by the leaves and therefore modifies leaf reflectance. Consequently, computing FMC from remote sensing data is more difficult than EWT, since two independent variables need to be estimated simultaneously (Bowyer & Danson, 2004; Ceccato et al., 2001).

A common approach to estimate FMC from satellite data has relied on empirical models, which establish local and species-oriented relations between field measured FMC and satellite derived reflectance or temperature. Most commonly those approaches are based on high-temporal resolution data, such as NOAA-AVHRR (Alonso et al., 1996; Chuvieco et al., 2003, 2004b; Garcia et al., 2008; Paltridge & Barber 1988; Vidal et al., 1994) or, more recently, MODIS (Dennison et al., 2005; Stow et al., 2005; Yebra et al., 2008b; Zarco-Tejada et al., 2003). These models have a known precision and are easily parameterized, but are difficult to generalize and apply operationally to large areas.

To overcome these limitations, several authors have proposed using radiative transfer models (RTM) to provide a more global approach for an operational estimation of water content worldwide (Ceccato et al., 2001, 2002; Fourty & Baret, 1997; Trombetti et al., 2008; Zarco-Tejada et al., 2003). These approaches are based on physical relations between water absorption and spectral reflectance,

* Corresponding author. Department of Geography, University of Alcalá, Calle Colegios 2, Alcalá de Henares, Madrid 28801, Spain.
E-mail address: marta.yebra@uah.es (M. Yebra).

0034-4257/$ – see front matter © 2009 Elsevier Inc. All rights reserved.
doi:10.1016/j.rse.2009.07.001

Author's personal copy

and therefore are independent of site conditions and do not require input field data. The water content is commonly estimated from inversion techniques, assigning to each observed spectrum the water content value of the most similar simulated spectrum.

In spite of their potential, the use of RTM for FMC estimation presents also several problems that make their operational application in fire risk assessment very complex. The main ones are the following:

1. They commonly estimate EWT rather than FMC, since the latter is not a direct parameter affecting light absorption. As previously said, FMC can be computed as a ratio of EWT and DM, and therefore can also be estimated from RTM providing that the contributions of DM and EWT to leaf reflectance can be properly separated (Danson & Bowyer, 2004; Riaño et al., 2005).
2. RTM are difficult to parameterize, since input parameters are very dependent on plant conditions (leaf chemistry, leaf area index, leaf angular distribution), as well as illumination and soil background. As many of those parameters are not available for particular regions or the simulation intends to cope with a wide diversity of study areas, commonly the required input parameters are allowed to vary randomly, within general or specific ranges. Typically, the latter provide better results, since adapted thresholds eliminate potential noise (Bowyer & Danson, 2004; Danson & Bowyer, 2004).
3. Closely connected with the former problem, the main difficulty in using RTM for FMC retrieval is the uncertainty of the inversion procedure. When searching for the most similar simulated spectrum to the observed one, a wide range of values can be retrieved, since very similar reflectances can be obtained from very different combinations of input parameters. This dilemma has been named the "ill-posed" inverse problem (Combal et al., 2002b). To reduce this problem, the modeller should provide simulation conditions as close as possible to what is expected, to avoid potential errors caused by unrealistic combinations of input parameters.

Several authors have tried to alleviate the impact of the "ill-posed" problem for the estimation of FMC. The most common alternatives have been the restriction of ranges of input parameters (Danson & Bowyer, 2004), and the removal of simulated spectra derived from unlikely combinations input parameters, based on field experience (Yebra et al., 2008b). This paper continues this effort and compares results of FMC estimation from inversion of RTM using on one hand random combinations of input parameters, and on the other, combinations based on ecological relations. The study is applied to Mediterranean shrublands in Spain, which are frequently affected by forest fires. Several plots were sampled in the field to assess the performance of random and ecologically oriented simulation approaches. MODIS collection 4 images were used as input data, following previous experience in this line of research (Yebra et al., 2008a,b).

2. Methods

2.1. Test sites and field data

Shrubland field sites were sampled in a wide range of ecological conditions within the Mediterranean region of Spain (Fig. 1 and Table 1). The first two plots were located 3 km apart in the Cabañeros National Park (central Spain) and were more intensively sampled, covering a 6 year series. These plots are mainly composed of *Cistus ladanifer* and *Phillyrea angustifolia*, two very common Mediterranean shrub species. Plots 3 and 4 are located around 150 and 250 km apart from Cabañeros, respectively. Both plots have similar species composition to the Cabañeros plots although P4 is dominated by *Rosmarinus officinalis* instead of *C. ladanifer*. Plots 5–12 are further from Cabañeros (between 270 and 700 km), shown as P7 in the border of the upper limit of the Mediterranean region. In species composition, these plots differ more from the Cabañeros site than the other plots.

All plots were sampled following the same standard protocol (Chuvieco et al., 2003) but in different years and time periods (Table 1). P1 and P2 were sampled from 2001 to 2007, every 16 days from April to September. Plots 3–7 were also sampled in the same seasons but only in 2 years (2001 and 2002), while plots 8–12 were only sampled twice in

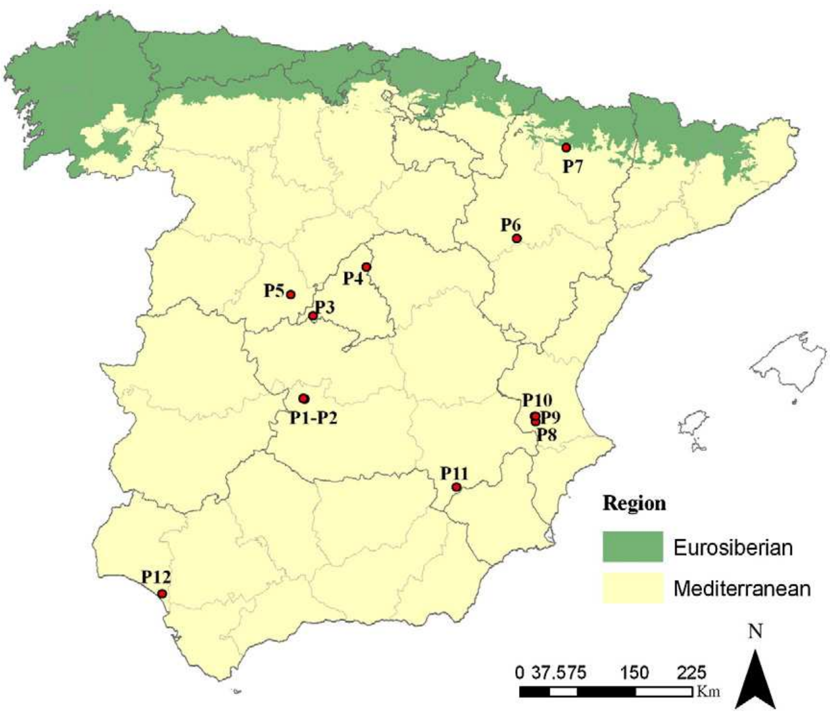

Fig. 1. Validation sites location (center coordinates recorded using GARMIN 12 GPS (5–10 m of error in *x* and *y*)).

Author's personal copy

Table 1
Overview of the field sampling and precise species composition of each site.

Code	Species composition (fcover %)	Period	Years	Sampling dates
P1	*Cistus ladanifer* (54%) *Phillyrea angustifolia* (25%) *Erica australis* (14%) *Rosmarinus officinalis* (7%)	April–September	2001–2005 and 2007	63
P2	*Cistus ladanifer* (57%) *Phillyrea angustifolia* (22%) *Erica australis* (16%) *Rosmarinus officinalis* (5%)	April–September	2001–2005 and 2007	63
P3	*Cistus ladanifer* (60%) *Rosmarinus officinalis* (40%)	April–September	2001–2002	24
P4	*Rosmarinus officinalis* (60%) *Cistus ladanifer* (40%)	April–September	2001–2002	24
P5	*Retama sphaerocarpa* (90%) *Lavandula stoechas* (10%)	April–September	2001–2002	24
P6	*Ulex parviflorus* (30%) *Thymus vulgaris* (30%) *Lavandula angustifolia* (30%) *Retama sphaerocarpa* (10%)	April–September	2001–2002	20
P7	*Genista scorpius* (40%) *Auercus coccifera* (20%) *Juniperus communis* (20%) *Rosmarinus officinalis* (20%)	April–September	2001–2002	20
P8	*Quercus coccifera* (50%) *Juniperus oxycedrus* (40%) *Cistus albidus* (10%)	April and July	2006	2
P9	*Ulex parviflorus* (80%) *Cistus albidus* (10%) *Rosmarinus officinalis* (5%) *Juniperus oxycedrus* (5%)	April and July	2006	2
P10	*Cistus albidus* (70%) *Ulex parviflorus* (20%) *Juniperus oxycedrus* (5%) *Rosmarinus officinalis* (5%)	April and July	2006	2
P11	*Juniperus phoenicea* (40%) *Juniperus oxycedrus* (35%)	April and July	2006	2
P12	*Erica arborea* (100%)	April	2006	1

2006; spring (10–12 of April) and summer (25–27 July). At each sampling plot and date two samples of live leafy material as well as small terminal branches were taken from several random fresh leaf shoots of each dominant species within a 900 m^2 area. The time of the sampling was from 12 a.m. to 4 p.m., when the fire risk is expected to be maximum and the FMC minimum (Castro et al., 2006).

The collected samples were immediately sealed, weighed on site (fresh weight, W_f) and then transported to the laboratory, oven-dried for 48 h at 60 °C, and weighed again (dry weight, W_d). FMC was computed as:

$$\text{FMC}\ (\%) = \frac{W_f - W_d}{W_d} \times 100. \tag{1}$$

Afterwards, average values of the FMC obtained per species, plot, and date were calculated and the representative value of FMC for each plot was finally computed as the mean FMC value of the species sampled, weighted according to their fraction of cover. FMCs of P1 and P2 were averaged together due to the proximity and similarity of these two plots.

2.2. Models used for FMC retrieval

The PROSPECT leaf optical properties model (Jacquemoud, 1990) and SAILH canopy reflectance model (Kuusk, 1985), were selected to retrieve FMC using inversion techniques. Both are well known models, widely used in recent literature (Jacquemoud et al., 2009).

PROSPECT simulates both leaf reflectance and transmittance over the solar spectrum (400–2500 nm) as a function of the chlorophyll a+b content (C_{a+b}), the equivalent water thickness (EWT), the dry matter content (DM) and the leaf structural parameter *N*. Since FMC is the percentage weight of water per unit of dry matter weight, it can be estimated from PROSPECT parameters (FMC = EWT/DM).

SAILH is a derivative version of SAIL (*Scattering by Arbitrary Inclined Leaves*) (Verhoef, 1984) which corrects the hot-spot effect (Kuusk, 1991.), with a new parameter which relates the leaf size and canopy height. Consequently, SAILH simulates canopy reflectance from the hot-spot parameter (*h*) as well as the leaf area index (LAI), the leaf angle distribution (LAD), the soil reflectance, the viewing and illumination conditions (the sun and view zenith angle, the relative azimuth sensor-sun angle and the atmospheric transmissivity) and the leaf reflectance and transmittance.

The linking between the two models (named PROSAILH) has been used for about 16 years to retrieve canopy biophysical variables (Jacquemoud et al., 2009) not only in homogeneous covers such as crops (Combal et al., 2002a; Koetz et al., 2005) or grasslands (Yebra et al., 2008b) but also in vertically heterogeneous canopies such as shrublands and woodlands (Colombo et al., 2008; Trombetti et al., 2008; Zarco-Tejada et al., 2003, 2004). Two consecutive phases were carried out to estimate FMC from MODIS and PROSAILH: (i) parameterization of PROSAILH and forward modeling and (ii) model inversion, based on the previously generated Look Up Table (LUT).

2.2.1. Parameterization of PROSAILH and forward modelling

Two different parameterizations were used in this paper. To compare the performance of the ecological simulation approach with the more traditional use of RTM, a first simulation scenario was build by randomly combining the input values within the ranges observed in the field. A uniform distribution was assumed for all of them (Table 2). This simulation scenario included a total of 63,504 spectra. It will be named random LUT (LUT_R) throughout the paper.

Table 2
Input parameters used for the simulations (ecological and random scenarios).

Scenario	Obs.	*N* (unitless)	C_{a+b} (µg/cm^2)	EWT (g/cm^2)	DM (g/cm^2)	LAD	Soil
Ecological	1	1.5	82.94	0.0316	0.0251	Planophile	Normal
	2	1.5	63.21	0.0263	0.0247	Planophile	Normal
	3	3	51.84	0.0297	0.0346	Planophile	Normal
	4	2	70.46	0.0223	0.0295	Erectophile	Dry
	5	3.5	51.24	0.0182	0.0360	Planophile	Dry
	6	3.5	48.79	0.0157	0.0352	Erectophile	Dry
	7	1.5	82.17	0.0219	0.0242	Plagiophile	Normal
	8	1	79.37	0.0290	0.0225	Plagiophile	Normal
	9	1.5	66.52	0.0270	0.0199	Plagiophile	Normal
	10	1.5	91.50	0.0231	0.0202	Erectophile	Dry
	11	1.5	66.00	0.0170	0.0170	Erectophile	Dry
	12	2	48.24	0.0179	0.0209	Plagiophile	Dry
	13	1	51.50	0.0197	0.0227	Plagiophile	Dry
	14	1.5	51.39	0.0180	0.0158	Plagiophile	Normal
	15	2	50.29	0.0181	0.0293	Plagiophile	Normal
	16	2	53.93	0.0091	0.0193	Erectophile	Normal
	17	2.5	42.20	0.0163	0.0270	Erectophile	Dry
	18	2.5	54.83	0.0124	0.0253	Erectophile	Dry
	19	2.5	37.64	0.0103	0.0224	Erectophile	Dry
	20	1.5	63.00	0.0072	0.0141	Plagiophile	Normal
	21	2	53.63	0.0160	0.0184	Plagiophile	Normal
	22	1.5	55.88	0.0136	0.0153	Plagiophile	Normal
	23	1.5	58.23	0.0136	0.0136	Plagiophile	Dry
	24	2	26.00	0.0170	0.0170	Erectophile	Dry
	25	2	49.15	0.0147	0.0180	Erectophile	Dry
	26	2	50.11	0.0152	0.0171	Erectophile	Dry
Random	Maximun	3.5	91.5	0.0316	0.036	Plagiophile	Normal & Dry
	Minimun	1	26	0.0072	0.0136		
	Step	0.5	13	0.005	0.004		

Author's personal copy

The ecological simulation scenario was built upon previous field experience in Mediterranean shrublands. Seasonal trends in biophysical parameters were considered, as well as variations between dry and wet years, and the different drought strategies of vegetation functional types (deciduous or perennial leaves). From these conditions, 26 specific combinations of parameters were input into the PROSPECT model (Table 2). The values were derived from field measurements in the Cabañeros National Park (Yebra et al., 2008b). The measurements were performed in two typical Mediterranean shrub species belonging to two different functional types; *C. ladanifer* (summer semi-deciduous drought-avoider shrub with an accompanying water spending strategy) and *P. angustifolia* (an evergreen sclerophyllous drought-tolerant shrub). The data were taken about every sixteen days during both dry and wet years (2005 and 2007, respectively).

At canopy level, each of the 26 combinations of leaf parameters was assigned a theoretical LAD according to the re-orientation that leaves experience as a strategy to decrease the light intercepted and the water stress (changes of LAD from planophile to erectophile) (Valladares & Pugnaire, 1999; Werner et al., 1999) (Table 2). A reference soil spectrum was selected from our own measurements with a GER2600 spectro-radiometer (GER Corp., Millbrook, NY), correcting between the spring and summer brightness (Koetz et al., 2005). The hot-spot was fixed throughout all the simulations at 0.001 as previously performed by Zarco-Tejada et al. (2003) as well as the viewing geometry (sun zenith angle = 30°, nadir angle = 0° and azimuth angle = 0°).

The LAI was assumed to follow a uniform distribution within a range of 0.5–2.5. This range was set from field measures in Mediterranean shrublands (Yebra & Chuvieco, 2008). 520 sets of input parameters were computed by randomly combining the 26 leaf-level combinations of parameters with LAI values (26 × 20). Some of those combinations were eliminated as they were very unlikely. Finally, a total of 275 combinations of PROSAILH parameters were used to run the models and 275 spectra over the range 400–2500 nm were simulated (Fig. 2). These spectra were linearly mixed with their soil spectra (normal or dry) in a proportion of 40%. The objective was to account for the fraction of vegetation/soil cover in the simulated reflectance, assuming that the global radiance of a pixel is proportional to the surface occupied for vegetation and soil. A total of 275 spectra were generated, with FMC values ranging from 44.6% to 135.68%. Throughout the paper, this simulation will be named ecological Look Up Table (LUT_E).

Some of the leaf parameters of LUT_E showed a statistically significant relationship between them. There was a weak relationship between EWT and C_{a+b} ($r = 0.45$, $p < 0.05$) and EWT and DM ($r = 0.47$, $p > 0.05$) while there was no significant relationship between DM and C_{a+b} ($r = -0.046$, $p = 0.8$).

The LUT_R showed a wider range of FMC values (228.57–19.34%) than the LUT_E, since no restriction to combinations of input parameters was applied. No significant correlations were found between parameters.

2.3. MODIS input data

Input data for the RTMs inversion was the 8-day composite MODIS/Terra product of surface reflectance at 500 m of spatial resolution (MOD09A1v004, (Vermote et al., 1997). This composite consists of seven bands centred at 857, 645, 469, 555, 1240, 1640 and 2130 nm and six additional bands indicating viewing geometry, state information, and atmospheric conditions. All spectra of both LUT_E and LUT_R were convolved to these seven MOD09A1 reflectance bands using the sensor response function.

The Terra-MODIS images over Spain are captured between 11 a.m. and 1 p.m. (http://earthobservatory.nasa.gov/MissionControl/overpass.html, February 2009), which is earlier than field sampling. However, this set of images were used instead of the Aqua-MODIS composites (MYD09A1 product), which are acquired between 1 p.m. and 3 p.m., since the Terra-MODIS images have a longer time series. Additionally, several studies have showed good correlations between reflectance data of Terra-MODIS and FMC measured on shrublands at the central hours of the day (Dennison et al., 2008; Roberts et al., 2006; Stow & Niphadkar 2007; Stow et al., 2005; Yebra et al., 2008b).

Besides the reflectance product, the Terra-MODIS LAI product MOD15A2v004 (Myneni et al., 2000) was also used in this paper to improve model inversion. This product is an 8-day composite of LAI and fractional photosynthetically active radiation (FPAR) at 1 km of spatial resolution.

Both MOD09A1 and MOD15A2v004 composites corresponding to the field sampling dates were acquired from the Land Processes Distributed Active Archive Center (https://wist.echo.nasa.gov/api/, February 2009) and reprojected from sinusoidal to UTM 30 T Datum European 1950 (ED50) using the nearest neighbour interpolation resampling. Additionally, MOD15A2 imagery was resampled to a spatial resolution of 500 m. The information of those images was extracted from each composite image using the median value of window adapted to the shape of shrub patches as recommended by Yebra et al. (2008b).

2.4. Model inversion

The inversion method used to retrieve FMC from MODIS was based on finding which of the simulated spectra was more similar to each of the observed spectra. Instead of iteratively computing the model for each pixel, this inversion technique only searches within the previously computed spectra (stored in the LUT). Therefore, it is very efficient in computation time and makes it possible to create user-oriented simulation scenarios that may follow more realistic assumptions (Combal et al., 2002b; Liang, 2004).

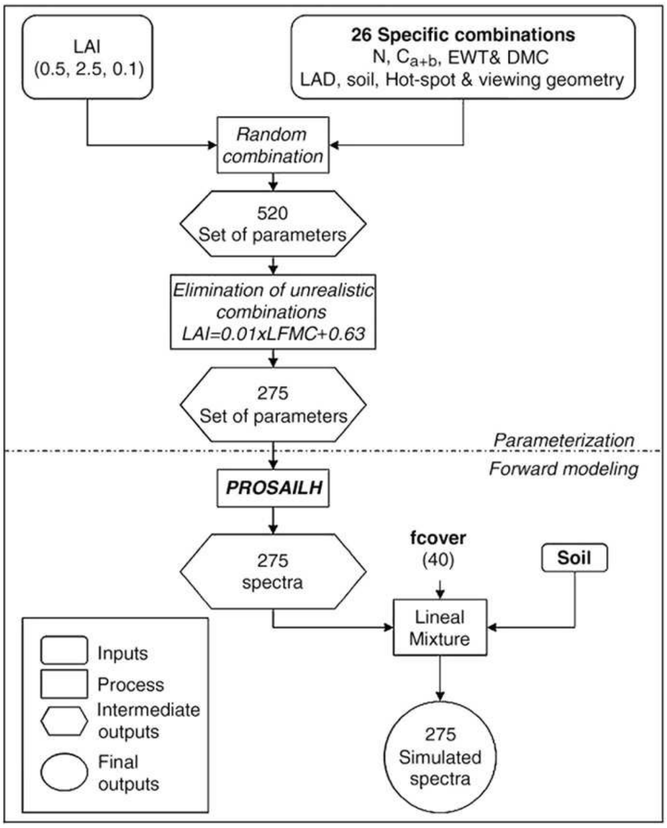

Fig. 2. Overview of the inputs and processes to generate the simulated data (ecological scenario).

Author's personal copy

The comparison between observed and simulated spectra is commonly based on defining a merit function that minimizes either the square error (Koetz et al., 2005; Zarco-Tejada et al., 2003), the simple root means square error (Combal et al., 2002b) or the relative root mean square error (Weiss et al., 2000).

In this paper, the spectral angle (SA, in radians) between the simulated and observed spectra was used:

$$\mathrm{SA}\left(\vec{v},\vec{w}\right) = \cos^{-1}\left(\frac{\vec{v}\times\vec{w}}{||\vec{v}||\times||\vec{w}||}\right) \tag{2}$$

where $\vec{v}$ and $\vec{w}$ are two vectors (observed and simulated, respectively) of m dimension, m being the number of bands considered for the classification.

The SA was first used as a merit function by De Santis and Chuvieco (2007) using Landsat–TM images and a set of simulated spectra derived from PROSPECT and Kuusk (Kuusk, 2001) to map burn severity. The authors considered the SA appropriate for the inversion because it is insensitive to illumination or albedo effects and can be operatively applied to a whole image.

To operatively carry out the inversion based on the SA, the Spectral Angle Mapper supervised classification technique (SAM, Kruse et al., 1993) implemented in ENVI 4.2™ image analysis commercial software was applied to MODIS imagery. Both sets of simulated spectra, $\mathrm{LUT_E}$ and $\mathrm{LUT_R}$, previously converted to a spectral library, were used as endmembers.

All MOD09A1 reflectance bands but number 5, which had radiometric problems[1], were used as input for the SAM classification. LAI values extracted from MOD15A2 were also used since several authors have showed improvements in water content estimation when LAI is fixed to a known value (Yebra, 2008; Zarco-Tejada et al., 2003). This is due to the fact that indetermination problems derived from compensations between LAI and FMC values are avoided.

2.5. Assessment

In order to evaluate the accuracy of the estimation, predicted FMC values ($\mathrm{FMC_P}$) were compared with the ground-measured FMC ($\mathrm{FMC_{Obs}}$) from each study site. The Pearson's correlation coefficient (r) or its square, the coefficient of determination (R^2) are commonly chosen for this purpose. However various studies have demonstrated that these coefficients are not necessarily related to the accuracy of predictions; where accuracy is defined as the degree to which $\mathrm{FMC_P}$ approach the magnitudes of their observed counterparts (Willmott, 1982). Following recommendations of Willmott (1982) the following summary measures were calculated and reported to quantitatively evaluate PROSAILH inversion performance:

1. Average and standard deviation of $\mathrm{FMC_P}$ ($\overline{\mathrm{FMC}}_\mathrm{P}$ and $\mathrm{SD_P}$) and $\mathrm{FMC_{Obs}}$ ($\overline{\mathrm{FMC}}_\mathrm{Obs}$ and $\mathrm{SD_{Obs}}$).
2. The intercept (a) and slope (b) of the least-squares regression $\mathrm{FMC_P} = a + b \times \mathrm{FMC_{Obs}}$.
3. The root mean square error (RMSE), which summarizes the difference between the $\mathrm{FMC_{Obs}}$ and $\mathrm{FMC_P}$ and indicate the average error of the estimations. This RMSE was separated into systematic (RMSEs) and unsystematic (RMSEu) portions. A good model is considered to have an unsystematic difference close to RMSE and the systematic difference close to zero.
4. The index of agreement (d). This index is both a relative and bounded measure which can be widely applied in order to make cross-comparisons between models. It takes values from 0 to 1 and it is defined as follows:

$$d = 1 - \left[\sum(\mathrm{FMC_P} - \mathrm{FMC_{Obs}})\hat{}^{2} \Big/ \left(|\mathrm{FMC'_P}| - |\mathrm{FMC'_{Obs}}|\right)\hat{}^{2}\right],$$

where $\mathrm{FMC'_P} = \mathrm{FMC_P} - \overline{\mathrm{FMC}}_\mathrm{Obs}$ and $\mathrm{FMC'_{Obs}} = \mathrm{FMC_{Obs}} - \overline{\mathrm{FMC}}_\mathrm{Obs}$.

The validation exercise was first carried out pooling all available data together in order to see the global performance of the model inversion and later sorting them out into plots in order to verify the site-independence of the methodology developed in this paper. Results with both ecological ($\mathrm{LUT_E}$) and random ($\mathrm{LUT_R}$) were compared.

3. Results

3.1. Input data

There were 146 field data points used to compare with MODIS estimates (Table 3). $\mathrm{FMC_{Obs}}$ values for those plots and periods ranged from 187.03 to 42.78%. Plots 3, 4, 5 and 7 registered the highest $\mathrm{FMC_{Obs}}$ with maximum values higher than the maximum FMC established in $\mathrm{LUT_E}$. Besides registering high $\mathrm{FMC_{Obs}}$, Plot 4 also showed the highest minimum $\mathrm{FMC_{Obs}}$ so its standard deviation was the lowest. The remainder plots showed similar statistics between each other with a range of $\mathrm{FMC_{Obs}}$ within the values established in both $\mathrm{LUT_E}$ and $\mathrm{LUT_R}$.

Fig. 3 displays an example of the ecological simulation scenario, where the expected trends in reflectance while vegetation dries out are shown: an increase in bands 6 and 7 (SWIR), which are the most sensitive bands to water absorption in the solar spectrum (Danson et al., 1992), while an increase in bands 3, 4 and 1 (blue, green and red) occurs due to the impacts of water shortage on chlorophyll content and LAI (Hardy & Burgan, 1999).

3.2. Model inversion performance

The best estimations of FMC were obtained from the ecological simulation ($\mathrm{LUT_E}$). Although both LUTs showed regression equations equally close to 1:1 linear fitting (slope ~0 and intercept ~1), $\mathrm{LUT_E}$ yielded a root mean square error (RMSE) much lower and an index of agreement (d) much higher than $\mathrm{LUT_R}$ (Table 4). Additionally, the distribution of $\mathrm{FMC_P}$ was closer to the distribution of $\mathrm{FMC_{Obs}}$ when using $\mathrm{LUT_E}$, although the maximum $\mathrm{FMC_P}$ was a 51.35% lower than the maximum $\mathrm{FMC_{Obs}}$. This was expected to happen since the maximum FMC considered in the $\mathrm{LUT_E}$ was lower than the maximum $\mathrm{FMC_{Obs}}$ within all plots and dates. Excluding observations with higher FMC than the thresholds of $\mathrm{LUT_E}$ (135.68%), the ecological simulation performs even better with much lower RMSE and RMSEs than the random simulation. When focusing only on values below the moisture of extinction (105%), which is a critical value for fire risk assessment (Chuvieco et al., 2004a), the performance of $\mathrm{LUT_E}$ clearly surpasses

Table 3
Statistics of the $\mathrm{FMC_{Obs}}$ per plot; Max., maximum; Min., minimum, $\overline{\mathrm{FMC}}_\mathrm{Obs}$, average; $\mathrm{SD_{Obs}}$, standard deviation.

PLOT	Max.	Min.	$\overline{\mathrm{FMC}}_\mathrm{Obs}$	$\mathrm{SD_{Obs}}$	N
P1–P2	118.65	42.78	84.77	23.01	51
P3	187.03	49.04	92.34	43.61	19
P4	143.73	75.74	96.15	16.54	15
P5	155.77	74.53	110.28	27.90	19
P6	116.19	42.93	73.86	22.27	16
P7	168.81	52.73	113.06	36.78	17
P8–12	118.65	42.78	73.89	23.94	9
ALL	187.03	42.78	92.04	30.55	146

[1] For a detailed description of this problem check: http://landweb.nascom.nasa.gov/cgi-bin/QA_WWW/displayCase.cgi?esdt=MOD09&caseNum=JB_MOD09_01278&caseLocation=cases_data, September 2008). The problem has been solved in collection 5 data. However the composites needed for this study were not reprocessed at the time of the study.

Author's personal copy

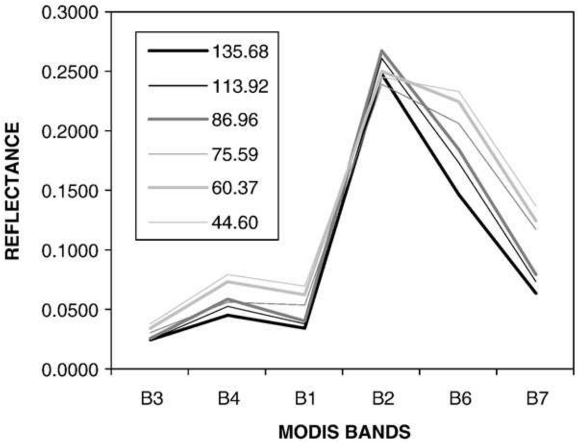

Fig. 3. Simulated MODIS reflectances corresponding to six FMC values randomly selected from the simulations. Band 5 is not represented because it was not used for the analysis.

that of LUT_R with one third of the errors and twice the index of agreement.

The better performance of LUT_E was also confirmed when looking at the result by sites (Table 5). Fist of all, LUT_R led to distributions of FMC_P further from distributions of FMC_{Obs} than LUT_E, regardless of which plot was being considered. Secondly, RMSE and d were in the range of 44.88 to 89.51% and 0.6 to 0.2 for LUT_R, respectively while ranging from 10.58% to 33.24% and 0.9 to 0.8 for LUT_E. Finally, LUT_R showed regression equations between FMC_P and FMC_{Obs} far from 1:1 in all plots but P4 while LUT_E, showed regression equations close to 1:1 in most of the plots.

Although LUT_E performed better than LUT_R, the earlier presented some inaccuracies in plots 3, 5 and 7. Plots 3 and 7 showed a regression equation far from 1:1 in both inversions. Additionally, their RMSE's were the highest, with RMSEs higher than RMSEu's. These inaccuracies appear to be related to systematic under-estimations caused by the threshold of simulation (where $FMC_{Obs}>135.68\%$). In addition, there are two dates (days 178 and 226 of 2002) where the FMC was highly over-estimated in P7 (Fig. 4), which may be caused by a field sampling error, since the data series does not have the logical evolution. Trends in P5 are more diverse between the two simulations, with good adjustments in LUT_E and rather poor in LUT_R.

The inversion model performance also showed certain inaccuracies in P4 since the regression equation was far from 1:1 while the RMSE lower than 15% and d 0.8. P4 registered the lower SD_{Obs}. This together with a systematic over-estimation of the range of FMC_{Obs} around 80% to values of 100% (Fig. 4) produced that regression equation far from 1:1.

4. Discussion and conclusions

This paper presents the potential of using ecological information to improve the parameterization of RTM to retrieve biophysical variables, and particularly the FMC. Simple random combinations of parameters render unrealistic combinations that very unlikely occur in nature. For instance, low moisture content values very unusually coincide with high chlorophyll values or low dry matter content (DM), since plants with water stress tend to reduce the photosynthetic activity and increase DM. Similarly, when input parameters in RTM are assumed to be fully independent, spurious combinations may produce similar reflectance characteristics to those derived from real situations, thus confusing the inversion process. The example shown in this paper offers evidence of this assertion, since field measured EWT was strongly correlated to C_{a+b} (along with FMC). These two parameters tend to decrease in conditions of water, temperature and radiation stress. Under high temperatures and greater radiation, the transpiration increases and consequently EWT decreases. Moreover, C_{a+b} absorbs too much energy compared with the photosynthetic capacity of the photosystem. That excess of energy that the photosystem cannot handle is highly damaging for the plant since it can produce irreversible photodamage to the photosynthetic apparatus or leaf abscission (Werner et al., 1999). Consequently plants adjust their photosynthesis capability by regulating the C_{a+b} of their leaves according to the seasonal need for dissipation of the excess of excitation energy (Chaves et al., 2002; Kyparissis et al., 2000; Valladares & Pugnaire, 1999).

On the other hand, Mediterranean shrubs increase DM with drought since higher DM reduces water loss by transpiration (Gratani & Varone, 2004b) and protect plants from photodamage (Castro-Díez et al., 1998; Clemente et al., 2005). Consequently both DM and C_{a+b} are closely related to EWT. The significance of these relations depends on the effectiveness of the increase in DM in avoiding water losses and protecting the photosynthetic apparatus, which in turn depends on the plant functional type. Increases of DM in drought semi-deciduous are not efficient enough to avoid water losses since they possess shallow roots systems and malacophyllous leaves with lower DM, making them more susceptible to drought (Bombelli & Gratani, 2003; Gratani & Varone, 2004b). Consequently EWT and C_{a+b} normally appears negatively and significantly correlated with DM. Conversely, evergreens shrubs usually have deeper root systems and sclerophyllous leaves (Gratani & Varone, 2004a) that help to avoid dehydration and photoinhibition. As a result neither EWT nor C_{a+b} is significantly correlated to DM. Since both functional types were mixed in our dataset, the correlations between EWT, DM, and C_{a+b} were weak. More significantly, the correlation between EWT and DM was the opposite of what we expected.

Much has been written concerning the many similarities between the vegetation of Mediterranean climatic regions of the world, communities such as the garrigue-maquis around the Mediterranean Sea, the chaparral of California, and the heath and mallee-broom-bush vegetation of southern Australia. This vegetation has many structural and phenological characteristics in common and all show similar life-form, physiological and morphological adjustments (Pierce et al., 1994).

This paper has presented an example of an approach that can be useful in operational studies. The results show that this approach should be applicable in other Mediterranean areas, but additional field sampling campaigns should be performed to improve our database of

Table 4
Quantitative measures of model inversion performance.

LUT	FMC	Max.	Min.	$\overline{FMC}_P$	SD_P	N	a	bx	RMSE	RMSEs	RMSEu	d
E	All	135.68	45.98	86.62	28.58	146	19.05	0.74	19.77	9.51	17.34	0.9
	<135.7	135.68	45.98	81.98	26.42	129	5.4	0.91	16.22	2.99	15.94	0.9
	<105	135.68	45.98	75.27	24.31	102	1.60	0.97	16.14	0.82	16.11	0.8
R	All	228.57	19.34	90.96	74.72	146	−19.26	1.2	64.93	6.3	64.63	0.6
	<135.7	228.57	19.34	82.58	69.68	129	−37.01	1.43	62.02	9.88	61.23	0.5
	<105	228.57	19.34	74.62	67.51	102	−51.42	1.66	60.91	12.36	59.64	0.4

E, ecological LUT; *R*, random LUT; FMC, live fuel moisture content (%); Max., maximum; Min., minimum; $\overline{FMC}_P$, average and SD_P, standard deviation of the predicted FMC; *a*, intercept and *b* slope of the least-squares regression; RMSE, root mean square error; RMSEs, RMSE systematic; RMSEu, RMSE unsystematic; *d*, index of agreement.

Author's personal copy

Table 5
Quantitative measures of FMC model performance by site.

LUT	PLOT	Max.	Min.	$\overline{FMC}_P$	SD_P	*a*	*b*x	RMSE	RMSEs	RMSEu	*d*
E	P1–P2	135.68	45.98	84.69	22.82	18.24	0.80	14.69	4.93	13.84	0.9
	P3	135.68	45.98	69.97	30.56	16.63	0.58	33.24	28.66	16.84	0.8
	P4	135.68	61.67	97.84	15.01	36.51	0.64	11.95	6.03	10.31	0.8
	P5	135.68	47.15	98.78	36.63	−16.64	1.05	24.44	11.57	21.52	0.8
	P6	106.48	45.98	68.97	24.63	−6.12	1.02	10.58	4.9	9.38	0.9
	P7	135.68	61.77	112.61	20.78	59.15	0.47	21.29	18.29	10.90	0.8
	P8–12	100	47.15	70.66	20.60	19.55	0.69	13.86	7.67	11.55	0.9
R	P1–P2	157.14	19.34	58.74	36.31	20.05	0.46	44.88	28.52	34.41	0.5
	P3	228.57	19.34	61.11	76.18	−28.27	0.97	69.18	31.25	61.72	0.6
	P4	228.57	32.71	141.12	83.25	2.72	1.44	89.51	45.52	77.07	0.2
	P5	228.57	19.34	149.85	93.51	−156	2.77	80.56	62.33	51.08	0.6
	P6	228.57	19.34	75.10	73.64	−27.49	1.39	65.26	8.48	64.71	0.4
	P7	228.57	60.77	128.64	57.47	114.25	0.13	65.31	34.31	55.58	0.4
	P8–12	228.57	19.34	84.96	78.36	−97.99	2.66	64.77	34.42	54.87	0.5

E, ecological LUT; *R*, LUT built by ranges; Max., maximum; Min., minimum; $\overline{FMC}_P$, average and SD_P, standard deviation of the predictions; *a*, intercept and *b* slope of the least-squares regression; RMSE, root mean square error (%); RMSEs, RMSE systematic (%); RMSEu, RMSE unsystematic (%); *d*, index of agreement.

variation of input parameters. In this regard, a further collaboration between remote sensing scientists with field ecologist would surely improve the retrieval of FMC and other biophysical parameters.

Results obtained from comparing field-measured FMC and those predicted using both LUT_E and LUT_R proved that a choice of co-occurring observed parameters provides better results, significantly decreasing the RMSE when compared to models run with unrestricted ranges. The results with LUT_E also improve with respect to previous studies which used less restricted ecological criteria, since contrary to Yebra (2008), the regression equation between FMC_P and FMC_{Obs} was close to 1:1 linear fitting (slope ~0 and intercept ~1), the RMSE was 5.41% lower than the error reported by Yebra et al. (2008b) and the systematic portion (RMSEs) was lower than the unsystematic (RMSEu). The RMSE of the estimation with LUT_E was also much lower than that reported by Colombo et al. (2008) when inverting PROSPECT using leaf level reflectance and transmittance data.

These advances in modeling FMC of the vegetation cover should provide a significant improvement to assess fire risk in Mediterranean environments from satellite images. Many authors have emphasized the importance of FMC to estimate fire ignition and propagation, since the amount of water in the vegetation is inversely related to ignition potential and rate of spread (Rothermel 1972; Catchpole & Catchpole 1991; Catchpole et al., 1999; Nelson, 2001). Moisture content directly affects the ignitability of leaves (Gill & Moore, 1996), which in turn affects the likelihood of plant ignition and initial fire spread (Pers. Comm. P. Zylstra, June 2009). Consequently, errors in FMC estimations may lead to erroneous predictions of fire risk and thereby affect the accuracy of decisions made by fire managers using remote sensing derived FMC (Dasgupta et al., 2007). In this regard, Dasgupta et al. (2007) analyzed the impact of FMC retrieval errors on fire spread predictions through a sensibility analysis performed using the FARSITE fire behavior model (Finney, 1998). The authors concluded that fire spread rates are very sensitive to FMC values below 100% in mature bushes. Below those values, a unit error in FMC retrieval can lead to an error of 0.84 m/h (meter/hour) in predicting no wind no-slope non-adjusted spread rate. When FMC values above 100%, the sensitivity decreases considerably with errors of

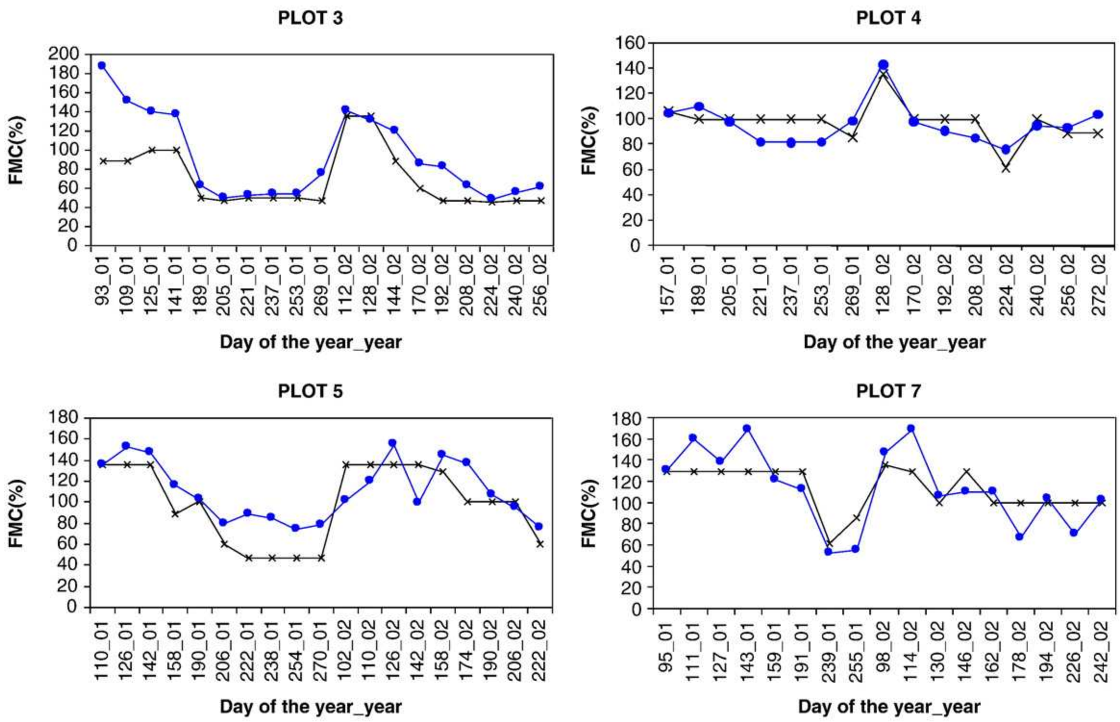

Fig. 4. Temporal evolution of FMC_P (dots) and FMC_{Obs} (crosses) of some plots.

Author's personal copy

0.0332 m/h per unit error in FMC. Consequently the improvement in the accuracy of the estimation of FMC showed in this study (44.77% for FMC values below 105%) may produce a significant improvement in predicting rate of spread in 37.6 m/h (44.77%*0.84 m/h), which is quite critical for fire managers. The effect of this improvement may be more substantial in multi-layered forests, where live fuel moisture plays an important role in the vertical development of fires into higher fuel strata (Pers. Comm. P. Zylstra, June 2009). The development of crown fires in coniferous forests for instance has been shown to be highly dependent on foliar moisture content (Van Wagner 1976, Alexander, 1996).

The limitations of our modeling approach are related to the conditions we initially stated or the input data used. The model under-estimates FMC values higher than 135.68%, which were actually the upper limit of our simulations. This is not very critical for fire danger estimation, since those FMC values are well above the moisture of extinction for Mediterranean species, so it is outside of the range where fire spread can be sustained (Chuvieco et al., 2004a). Nevertheless the models presented here can be used in other applications so simulation results are expected to be improved in future work by introducing in the model the spectra signatures of vegetation with FMC higher than 135.68%.

The second main limitation relates to the accuracy of the input data, particularly the standard MODIS LAI product (MOD15A2), which has been reported in previous studies (Knyazikhin et al., 1999). The quantitative impact on our results has not been evaluated here.

In future work, new methods for the retrieval of LAI will be investigated. Previous work has accurately estimated LAI with LIDAR (Riaño et al., 2007) or meteorological data (Koetz et al., 2005) so these alternatives will be explored.

In summary, this study has offered an example of the improvements in retrieval of biophysical parameters by linking ecological information and RTM, to improve the simulation scenarios. The ultimate cause of the “ill-posed” problem to retrieve biophysical parameters is the lack of ecological information in the RTM. RTM are based on physical relations between input parameters, but they assume that those parameters vary independently, which is not true in real plants. Chlorophyll variation is related to water, and water to dry matter, and all to LAI, since atmospheric and soil conditions affect the overall plant physiology. Therefore, physically-based models should be complemented with ecologically oriented models, thus reducing potential noises caused by unrealistic combination of parameters, which cause retrieval errors.

This paper has been focused on the estimation of FMC in Mediterranean shrublands in Spain, which are frequently affected by forest fires, but the same scheme should be applicable to other ecological regions.

Acknowledgements

This work was supported by the FIREMAP (CGL2004-060490C04-01/CLI) and FIREGLOBE (CGL2008-01083) projects, funded under the Spanish Ministry of Science and Technology. The authors gratefully acknowledge Héctor Nieto, María Díaz and Rubén Muñoz for their contribution in the field sampling campaigns and members of the FIRERISK project for their contribution in the data of 2001 and 2002 used in this study. Suggestions and comments from Philip Zylstra, fire technical officer of the Snowy Mountains Region (Australia) are also acknowledged.

References

Alexander, M. E. (1996). Crown fire thresholds in exotic pine plantations of Australasia. PhD thesis, University of NSW, Canberra: Australia.

Alonso, M., Camarasa, A., Chuvieco, E., Cocero, D., Kyun, I., Martín, M. P., et al. (1996). Estimating temporal dynamics of fuel moisture content of Mediterraneam species from NOAA-AVHRR data. *EARSEL Advances in Remote Sensing*, *4*, 9—24.

Bombelli, A., & Gratani, L. (2003). Interspecific differences of leaf gas exchange and water relations of three evergreen Mediterranean shrub species. *Photosynthetica*, *41*, 619—625.

Bowyer, P., & Danson, F. M. (2004). Sensitivity of spectral reflectance to variation in live fuel moisture content at leaf and canopy level. *Remote Sensing of Environment*, *92*, 297—308.

Castro, F. X., Tudela, A., Gabriel, E., Montserrat, D., Canyameres, E., & Segarra, M. (2006). Evolution of live fuel moisture in mediterranean forest. In D. X. Viegas (Ed.), *V International Conference on Forest Fire Research* : FIguera da Foz.

Castro-Díez, P., Villar-Salvador, C., Pérez-Rontomé, M., Maestro-Martínez, & Montserrat-Martí, G. (1998). Leaf morphology, leaf chemical composition and stem xylem characteristics in two Pistacia (Anacardiaceae) species along a climatic gradient. *Flora*, *193*, 195—202.

Catchpole, W. R., Bradstock, R. A., Choate, J., Fogarty, L. G., Gellie, N., McCarthy, G. J., et al. (1999). Cooperative development of prediction equations for fire behaviour in heathlands & shrublands. *Proc. Aust. Bushfire Conf., Albury: Australia*.

Catchpole, E. A., & Catchpole, W. R. (1991). Modelling moisture damping for fire spread in a mixture of live and dead fuels. *International Journal of Wildland Fire*, *1*(2), 101—106.

Ceccato, P., Flasse, S., & Gregoire, J. M. (2002). Designing a spectral index to estimate vegetation water content from remote sensing data: Part 2. Validation and applications. *Remote Sensing of Environment*, *82*, 198—207.

Ceccato, P., Flasse, S., Tarantola, S., Jacquemoud, S., & Grégoire, J. M. (2001). Detecting vegetation leaf water content using reflectance in the optical domain. *Remote Sensing of Environment*, *77*, 22—33.

Chaves, M. M., Pereira, J. S., Maroco, J., Rodrigues, M. L., Ricardo, C. P. P., Osorio, M. L., et al. (2002). How plants cope with water stress in the field? *Photosynthesis and growth* (pp. 907—916).

Cheng, Y. B., Zarco-Tejada, P. J., Riaño, D., Rueda, C. A., & Ustin, S. (2006). Estimating vegetation water content with hyperspectral data for different canopy scenarios: Relationships between AVIRIS and MODIS indexes. *Remote Sensing of Environment*, *105*, 354—366.

Chuvieco, E., Aguado, I., Cocero, D., & Riaño, D. (2003). Design of an empirical index to estimate fuel moisture content from NOAA-AVHRR analysis in forest fire danger studies. *International Journal of Remote Sensing*, *24*, 1621—1637.

Chuvieco, E., Aguado, I., & Dimitrakopoulos, A. (2004). Conversion of fuel moisture content values to ignition potential for integrated fire danger assessment. *Canadian Journal of Forest Research—Revue Canadienne De Recherche Forestiere*, *34*(11), 2284—2293.

Chuvieco, E., Aguado, I., Yebra, M., Nieto, H., Salas, J., Martín, M.P., et al. (in press). Development of a framework for fire risk assessment using remote sensing and geographic information system technologies. Ecological Modelling. doi:10.1016/j.ecolmodel.2008.11.017.

Chuvieco, E., Cocero, D., Riaño, D., Martín, M. P., Martínez-Vega, J., de la Riva, J., et al. (2004). Combining NDVI and surface temperature for the estimation of live fuel moisture content in forest fire danger rating. *Remote Sensing of Environment*, *92*, 322—331.

Clemente, A. S., Rego, F. C., & Correia, O. A. (2005). Growth, water relations and photosynthesis of seedlings and resprouts after fire. *Acta Oecologica*, *27*, 233—243.

Colombo, R., Meroni, M., Marchesi, A., Busetto, L., Rossini, M., Giardino, C., et al. (2008). Estimation of leaf and canopy water content in poplar plantations by means of hyperspectral indices and inverse modeling. *Remote Sensing of Environment*, *112*, 1820—1834.

Combal, B., Baret, F., & Weiss, M. (2002). Improving canopy variables estimation from remote sensing data by exploiting ancillary information. *Case study on sugar beet canopies*.

Combal, B., Baret, F., Weiss, M., Trubuil, A., Mace, D., Pragne're, A., et al. (2002). Retrieval of canopy biophysical variables from bidirectional reflectance using prior information to solve the ill-posed inverse problem. *Remote Sensing of Environment*, *84*, 1—15.

Danson, F. M., & Bowyer, P. (2004). Estimating live fuel moisture content from remotely sensed reflectance. *Remote Sensing of Environment*, *92*, 309—321.

Danson, F. M., Steven, M. D., Malthus, T. J., & Clark, J. A. (1992). High-spectral resolution data for determining leaf water content. *International Journal of Remote Sensing*, *13*, 461—470.

Dasgupta, S., Qu, J. J., Hao, X., & Bhoi, S. (2007). Evaluating remotely sensed live fuel moisture estimations for fire behavior predictions in Georgia, ISA. *Remote Sensing of Environment*, *108*, 138—150.

De Santis, A., & Chuvieco, E. (2007). Burn severity estimation from remotely sensed data: performance of simulation versus empirical models. *Remote Sensing of Environment*, *108*, 422—435.

Dennison, P. E., Roberts, D. A., & Peterson, S. H. (2008). Spectral shape-based temporal compositing algorithms for MODIS surface reflectance data. *Remote Sensing of Environment*, *109*, 510—522.

Dennison, P. E., Roberts, D. A., Peterson, S. H., & Rechel, J. (2005). Use of normalized difference water index for monitoring live fuel moisture. *International Journal of Remote Sensing*, *26*, 1035—1042.

Finney, M. A. (1998). *FARSITE fire area simulator version 1.0: Users guide and technical documentation.* Missoula, MT: Systems for Environmental Management.

Fourty, T., & Baret, F. (1997). Vegetation water and dry matter contents estimated from top-of-the atmosphere reflectance data: A simulation study. *Remote Sensing of Environment*, *61*, 34—45.

Garcia, M., Aguado, I., & Chuvieco, E. (2008). Combining AVHRR and meteorological data for estimating live fuel moisture content in forest fire danger rating. Remote Sensing of Environment, in review. *Remote Sensing of Environment*, 112, 3618–3627.

Gill, A. M., & Moore, P. H. R. (1996). Ignitability of leaves of Australian plants. *Contract report to the Australian Flora Foundation* Canberra: Australia: CSIRO Plant Industry.

Gratani, L., & Varone, L. (2004). Adaptive photosynthetic strategies of the Mediterranean maquis species according to their origin. *Photosynthetica*, *42*, 551—558.

Gratani, L., & Varone, L. (2004). Leaf key traits of *Erica arborea* L., *Erica multiflora* L. and *Rosmarinus officinalis* L. co-ocurring in the Mediterranean maquis. *Flora*, *199*, 56—69.

Author's personal copy

Hardy, C. C., & Burgan, R. E. (1999). Evaluation of NDVI for monitoring live moisture in three vegetation types of the Western U.S. *Photogrammetric Engineering and Remote Sensing*, *65*, 603−610.

Jacquemoud, S. (1990). PROSPECT: A model to leaf optical properties spectra. *Remote Sensing of Environment*, *34*, 74−91.

Jacquemoud, S., Verhoef, W., Baret, F., Bacour, C., Zarco-Tejada, P., Asner, G., et al. (2009a). PROSPECT + SAIL models: A review of use for vegetation characterization. *Remote Sensing of Environment, 113* (Supplement 1), S56–S66.

Knyazikhin, Y., Glassy, J., Privette, J. L., Tian, Y., Lotsch, A., Zhang, Y., et al. (1999). MODIS leaf area index (LAI) and fraction of photosynthetically active radiation absorbed by vegetation (FPAR) product (MOD15). *Algorithm theoretical basis document* http://eospso.gsfc.nasa.gov/atbd/modistables.html

Koetz, B., Baret, F., Poilvé, H., & Hill, J. (2005). Use of coupled canopy structure dynamic and radiative transfer models to estimate biophysical canopy characteristics. *Remote Sensing of Environment*, *95*, 115−124.

Kruse, F. A., Lefkoff, A. B., Boardman, J. B., Heidebrecht, K. B., Shapiro, A. T., Barloon, P. J., et al. (1993). The spectral image processing (SIPS) — Interactive visualization and analysis of imaging specrometer data. *Remote Sensing of Environment*, *44*, 145−163.

Kuusk, A. (1985). The hot spot effect of a uniform vegetative cover. *Soviet Journal of Remote Sensing*, *3*, 645−658.

Kuusk, A. (1991). The hot spot effect in plant canopy reflectance. In R. J. Myneni & R. B. (Eds.), *Photon vegetation interactions* (pp. 139−159). Springer-Verlag.

Kuusk, A. (2001). A two-layer canopy reflectance model. *Journal of Quantitative Spectroscopy & Radiative Transfer*, *71*, 1−9.

Kyparissis, A., Drilias, P., & Manetas, Y. (2000). Seasonal fluctuations in photoprotective (xanthophyll cycle) and photoselective (chlorophylls) capacity in eight Mediterranean plant species belonging to two different growth forms. *Functional Plant Biology*, *27*, 265−272.

Liang, S. (2004). *Quantitative remote sensing for land surface characterization.* Hoboken, NJ: Wiley.

Myneni, R., S.W, R., Glassy, J., & Votava, P. (2000). *FPAR, LAI user's guide.* (ESDT: MOD15A2) 8-day Composite.

Nelson, R. M. (2001). Water relations of forest fuels. In E. A. Johnson & K. Miyanishi (Eds.), *Forest fires: Behavior and ecological effects* (pp. 79−149). San Diego, Calif.: Academic Press.

Paltridge, G. W., & Barber, J. (1988). Monitoring grassland dryness and fire potential in Australia with NOAA/AVHRR data. *Remote Sensing of Environment*, *25*, 381−394.

Pierce, L. L., Running, S. W., & Walker, J. (1994). Regional-scale relationships of leaf area index to specific leaf area and leaf nitrogen content. *Ecological Applications*, *4*, 313−321.

Riaño, D., Chuvieco, E., Ustin, S. L., Salas, J., Rodríguez-Pérez, J. R., Ribeiro, L. M., et al. (2007). Estimation of shrub height for fuel type mapping combining airborne LiDAR and simultaneous color infrared ortho image. *International Journal of Wildland Fire*, *16*, 341−348.

Riaño, D., Ustin, S. L., Usero, L., & Patricio, M. A. (2005). Estimation of fuel moisture content using neural networks. *Artificial Intelligence and Knowledge Engineering Applications: A Bioinspired Approach, Pt 2, Proceedings*, *vol. 3562* (pp. 489−498).

Roberts, D. A., Peterson, S., Dennison, P. E., Sweeney, S., & Rechel, J. (2006). Evaluation of Aibone visible/infrared imaging spectrometer (AVIRIS) and moderate resolution imaging spectrometer (MODIS) measures of live fuel moisture and fuel condition in a shrubland ecosystem in southern California. *Journal of Geophysical Research*, *111*, GO4S02. doi:10.1029/2005JG000113

Rothermel, R. C. (1972). A mathematical model for predicting fire spread in wildland fuels. *USDA Forest Service research paper INT-115, Intermountain Forest & Range Experiment Station, Ogden, Utah*.

Stow, D., & Niphadkar, M. (2007). Stability, normalization and accuracy of MODIS-derived estimates of live fuel moisture for southern California chaparral. *International Journal of Remote Sensing*, *28*, 5175−5182.

Stow, D., Niphadkar, M., & Kaiser, J. (2005). MODIS-derived visible atmospherically resistant index for monitoring chaparral moisture content. *International Journal of Remote Sensing*, *26*, 3867−3873.

Trombetti, M., Riano, D., Rubio, M. A., Cheng, Y. B., & Ustin, S. L. (2008). Multi-temporal vegetation canopy water content retrieval and interpretation using artificial neural networks for the continental USA. *Remote Sensing of Environment*, *112*, 203−215.

Valladares, F., & Pugnaire, F. I. (1999). *Tradeoffs between irradiance capture and avoidance in semi-arid environments assessed with a crown architecture model* (pp. 459−469).

Van Wagner, C. E. (1976). Conditions for the start and spread of crown fire. *Canadian Journal of Forest Research*, *7*, 23−44.

Verhoef, W. (1984). Light scattering by leaf layers with application to canopy reflectance modeling: The SAIL model. *Remote Sensing of Environment*, *16*, 125−141.

Vermote, E. F., El Saleous, N. Z., Justice, C. O., Kaufman, Y. J., Privette, J. L., Remer, L., et al. (1997). Atmospheric correction of visible to middle-infrared EOS-MODIS data over land surfaces: Background, operational algorithm and validation. *Journal of Geophysical Research*, *102*, 17131−17141.

Vidal, A., Pinglo, F., Durand, H., Devaux-Ros, C., & Maillet, A. (1994). Evaluation of a temporal fire risk index in Mediterranean forest from NOAA thermal IR. *Remote Sensing of Environment*, *49*, 296−303.

Viegas, D. X., Viegas, T. P., & Ferreira, A. D. (1992). Moisture content of fine forest fuels and fire occurrence in central Portugal. *The International Journal of Wildland Fire*, *2*, 69−85.

Weiss, M., Baret, F., Myneni, R. B., Pragnère, A., & Knyazikhin, Y. (2000). Investigation of a model inversion technique to estimate canopy biophysical variables from spectral and directional reflectance data. *Agronomie*, *20*, 3−22.

Werner, C., Correia, O., & Beyschlag, W. (1999). Two different strategies of Mediterranean macchia plants to avoid photoinhibitory damage by excessive radiation levels during summer drought. *Acta OEcologica*, *20*, 15−23.

Willmott, C. J. (1982). Some comments on the evaluation of model performance. *Bulletin of the American Meteorological Society*, *63*, 1309−1313.

Yebra, M. (2008). Estimación del contenido de humedad de vegetación mediterránea a partir de imágenes MODIS. *Departamento de geografía* (pp. 202). Alcala de Henares: Universidad de Alcala.

Yebra, M., & Chuvieco, E. (2008). Modelos de simulación de reflectividad en ecología: potencialidades y problemas. *Ecosistemas*, *17*, 23−38.

Yebra, M., Chuvieco, E., & Aguado, I. (2008). Comparación entre modelos empíricos y de transferencia radiativa para estimar contenido de humedad en pastizales: Poder de generalización. *Revista de Teledetección*, *29*, 73−90.

Yebra, M., Chuvieco, E., & Riaño, D. (2008). Estimation of live fuel moisture content from MODIS images for fire risk assessment. *Agricultural and Forest Meteorology*, *148*, 523−536.

Zarco-Tejada, P., Miller, J. R., Morales, A., Berjón, A., & Agüera, J. (2004). Hyperspectral indices and model simulation for chlorophyll estimation in open-canopy tree crops. *Remote Sensing of Environment*, *90*, 463−476.

Zarco-Tejada, P. J., Rueda, C. A., & Ustin, S. L. (2003). Water content estimation in vegetation with MODIS reflectance data and model inversion methods. *Remote Sensing of Environment*, *85*, 109−124.